ELSEVIER

Materials Science and Engineering B 124–125 (2005) 283–287

MATERIALS SCIENCE & ENGINEERING B

www.elsevier.com/locate/mseb

Positron annihilation studies of high dose Sb implanted silicon

H. Schut[a,*], S.W.H. Eijt[a], C.D. Beling[b], K. Ho[b], Y. Takamura[c]

[a] *Department of Radiation, Radionuclides & Reactors, Faculty of Applied Sciences, Delft University of Technology, Mekelweg 15, NL-2629 JB Delft, The Netherlands*
[b] *Department of Physics, University of Hong Kong, Pokfulam Road, Hong Kong, PR China*
[c] *University of California, Berkeley, Berkeley, CA 94720, USA*

Abstract

The formation and evolution of vacancies and precipitates created by implantation of 60 keV, $2 \times 10^{16}\,cm^{-2}$ Sb^{+} in pre-amorphized (0 0 1) Cz–Si is studied using the Doppler broadening (DB) and two-dimensional angular correlation of annihilation radiation (2D-ACAR) positron beam techniques. After implantation, samples were laser annealed (LTA) and subsequently thermal annealed at temperatures ranging from 400 to 1000 °C. Implantation-induced vacancy-type defects were detected up to a depth of 280 nm. After LTA, positron annihilation related to both Sb and remaining defects is observed in the first 100 nm below the surface. The deeper region only shows positron trapping at vacancy-type defects with strong reduced concentration. Complete removal is obtained after 600 °C anneal. At this temperature, the positron data for the upper region reveals trapping at Sb and Si sites only. With increasing annealing time (at 600 °C) or increasing temperature (up to 1000 °C) positron annihilation at Sb-sites associated with neighboring vacancies becomes apparent. Results are correlated with the observed Sb electrical deactivation above 600 °C, the shift from small Sb aggregates to precipitates and out-diffusion of Sb from the implantation region at higher temperatures.

Keywords: Positron annihilation; Ion implantation; Laser annealing; Electrical deactivation; Precipitates; Antimony

1. Introduction

The challenge in manufacturing faster silicon semiconductor integrated circuits lies in the simultaneous reduction of the junction depth and sheet resistance while increasing the junction abruptness [1]. High dose, low energy ion implantation is considered as the technique to meet these requirements. However, in order to remove implantation-induced defects and to electrically activate the dopant atoms a subsequent thermal anneal step is required. As the conventional rapid thermal annealing (RTA) has reached its application limits, the alternative method of laser thermal annealing (LTA) is being explored intensively [2–4]. A complicating side effect of this method is the observed electrical deactivation upon further thermal annealing of the metastable, supersaturated dopant concentrations. In case of antimony doping this has been tentatively attributed to the formation of new inactive structures in the form of Sb aggregates and precipitates [5].

In this study we have applied positron beam annihilation techniques (Doppler broadening and 2D-ACAR) to investigate the behavior of Sb implantation induced defects and the evolution of Sb precipitates or clusters formed during the subsequent LTA and thermal annealing treatments. For a detailed description of positron annihilation studies in semi-conductors (see [6]).

2. Experimental

2.1. Sample preparation

(0 0 1)-Oriented Czochralski silicon wafers were pre-amorphised by implantation of $1 \times 10^{15}\,cm^{-2}$ Si ions at 55 keV. Next the implantation of the Sb dopant at 60 keV to a dose of $2 \times 10^{16}\,cm^{-2}$ was carried out. The laser annealing was performed at Verdant Technologies on a frequency doubled Nd:YAG laser operating at 532 nm with a FWHM of the laser pulse fixed at 14 ns. Laser fluences of $0.73\,J/cm^2$ with 10 shots at each location were used resulting in melt depths of 110 nm [2]. These melt depths are considered sufficient to repair all the damage of the previous implants including so-called end of range (EOR) defects that extend below the amorphous-crystalline interface. From SIMS measurements [4] box shaped dopant profiles were derived with Sb concentrations of $2.2 \times 10^{22}\,cm^{-3}$, which is well above the maximum Sb

* Corresponding author. Tel.: +31 15 2 781961; fax: +31 15 2 786422.
E-mail address: hschut@iri.tudelft.nl (H. Schut).

0921-5107/$ – see front matter
doi:10.1016/j.mseb.2005.08.011

solubility of 7×10^{19} cm^{-3} at 1300 °C. The implanted and LTA treated wafers were diced into 5×5 mm squares and a low temperature oxide, serving as capping preventing the outdiffusion of dopants, was deposited using LPCVD at 300–350 °C. After removal of the oxides, samples were subsequently thermally annealed at 600 °C for 30 s or between 400 and 1000 °C for 300 s in vacuum at Delft University. Hall effect measurements indicated that after LTA the active dopant concentration amounts to 60–70% [5].

2.2. Positron annihilation techniques

To monitor the behavior of defects after the pre-amorphization and dopant implantations and to study the evolution of precipitates or clusters formed during the subsequent LTA and thermal annealing treatments, the one and two-detector Doppler broadening (DB) and two-dimensional angular correlation of annihilation radiation (2D-ACAR) techniques are applied. Both techniques utilize a beam of mono-energetic positrons with energies tunable between 100 eV and 25 keV. This offers the possibility to choose the depth at which the positrons become thermalized and subsequently annihilate. The relation between the implantation energy and the mean implantation depth for positrons injected into silicon is shown by the bottom and top axes of Fig. 1. After implantation and thermalization the positron diffuses through the matrix until it annihilates with an electron as a free positron or it becomes trapped in a defect or at a precipitate. In the zero momentum frame the ultimate annihilation results in the emission of two collinear photons each with energy equal to 511 keV ($=m_0c^2$). In the laboratory frame the measured energy of the annihilation photons deviates from 511 keV by an amount equal to $-1/2E_{\rm B} \pm 1/2p_zc$, with p_z the electron momentum component parallel to direction of photon emission and $E_{\rm B}$ the binding energy of the electrons to the solid. The perpendicular components (p_x, p_y) cause a small angular deviation from collinearity between the two simultaneously emitted photons given by $\phi = p_y/m_0c$ and $\theta = p_x/m_0c$.

In a single detector DB-spectrum the electron momentum component p_z leads to a broadening of the 511 keV photo-peak. It is common practice to quantify the broadening by two parameters, *S* and *W*. The *S*(*hape*) parameter is defined as the ratio of counts accumulated in the central part of the photo-peak to the total peak contents and relates to annihilations with low momentum valence or conduction electrons. The *W*(ing) parameter (proportional to the counts accumulated in the high and low energy regions of the photo-peak) reflects the annihilations with high momentum core electrons. As an example, positrons trapped in Si vacancies have a higher probability to annihilate with low momentum valence electrons than with core electrons and therefore an increase in *S* is observed when compared to annihilations at interstitial sites. Since core electron orbitals are element specific the *W* parameter can be used to distinguish between annihilations at element specific sites. As an example, the normalized *S*,*W* cluster points for Si and Sb measured at single crystals are shown in Fig. 2.

A higher sensitivity for core electron annihilation events is obtained when both annihilation photons are detected in time coincidence using two Ge detectors aligned with the sample. By correlating the energies of the two photons (with Doppler shifts of $+1/2p_zc$ and $-1/2p_zc$) the signal to background ratio is increased to five orders of magnitude. This enhanced performance allows the construction of measured momentum distributions as linear combinations of the distributions obtained for the pure elements [7] or the direct comparison with calculated momentum distributions [8,9]. The two detector spectra shown in this study are measured at 3 keV positron implantation energy.

Analysis of the measured *S*(*E*) and *W*(*E*) curves as shown in Fig. 1 is done with the fitting and modeling program VEPFIT [10]. It solves the time averaged (positron) diffusion equation, taking into account the positron implantation profile, depth dependent positron diffusion and trapping and electric field

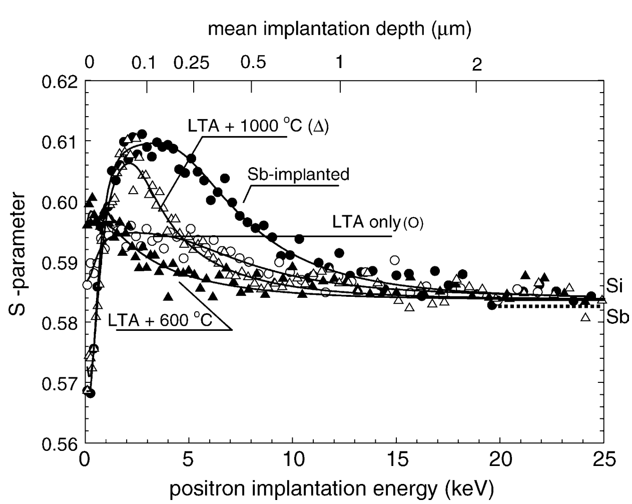

Fig. 1. The Doppler broadening *S*-parameter as a function of the positron implantation energy (bottom axis) and mean positron implantation energy (top axis). Data is shown for: amorphization followed by Sb implantation (●), LTA (○), LTA + 600 °C (30 s) thermal annealing (▲) and LTA + 1000 °C (300 s) (△). Values for Sb and Si single crystals are indicated on the right. The lines represent the result obtained by VEPFIT.

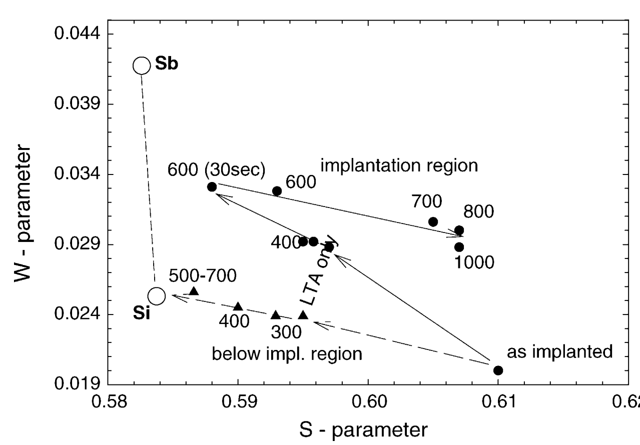

Fig. 2. Map of fitted *S* and *W* Doppler parameters for Sb implanted samples and Sb and Si single crystals. The different sample treatments are indicated. The numbers indicate the thermal annealing temperature (°C, annealing time 300 s). The triangular symbols represent the data obtained for depths below the implantation region.